

Report for ESRF Experiment MA-1406

Fabrication of complex Au/ α -Fe₂O₃ nanoparticles by thin films deposition and annealing

In this work we present a new method to obtain complex nanoparticles (NPs) by thin films deposition and annealing in air. We used this method to fabricate ensembles of Au/ α -Fe₂O₃ NPs over silica substrates. Thermal treatments promote the modifications of the deposited films toward the formation of complex nanoparticles. The nanostructures morphology can be tuned through the preparation parameters as films initial thickness, annealing temperature and time. With this method, two different routes are proposed to obtain these nanoparticles tuning their interaction and controlling the formation of dimmers.

It is well known that NPs exhibit different properties than bulk materials with the same chemical composition due to size, surface and proximity effects^{1,2}. Therefore, these nanomaterials offer the possibility to tune their physical properties by controlling size, shape or aggregation states, yielding many applications in different fields^{1,3,4}. Complex NPs as core-shell, nano-agglomerates or nanodimers, exhibit further advantages since they combine the properties of their individual components with additional ones arising from their interaction because of interface and proximity effects^{3,5}. The fabrication of simple (i.e., with a single phase) NPs by chemical or physical routes is well established. It is possible to obtain large amounts of NPs at reasonable cost and with a good control of their size, shape or aggregation⁶. However, fabrication of complex NPs is still an open issue not completely solved. Both chemical and physical methods have shown their ability to obtain these complex nanostructures^{7,8,9}, but with a high cost and low production efficiency. Hence, the fabrication of large amount of complex nanoparticles at economically viable costs is a milestone in the development of nanotechnology.

A well known method to obtain large amounts of NPs dispersed over a substrate consists on the deposition of a metallic thin film and a consequent annealing^{10,11}. During the cooling processes, the difference in thermal expansion coefficient between the film and the substrate induces mechanical stresses. As a result, the metallic film undergoes morphological modifications in order to relax this stress: formation of hillocks, holes nucleation and subsequently agglomeration leading to the formation of nanostructures^{10,12}. The morphology and size of these nanostructures depends on different parameters as the film initial thickness and annealing conditions (time, temperature, atmosphere and heating/cooling ramp), providing a method to tune the nanostructures features modifying any of these parameters¹³. This phenomenology was initially considered as a problem in the fabrication of microelectronic devices but it

has been recently used successfully to obtain noble metal nanoparticles. Few works explored the possibility to use it with other metals ^{13-14,15}. However, up to our best knowledge, it has never being applied to obtain complex nanoparticle with more than one phase.

In this work, we address the fabrication of complex NPs over silica substrates by deposition of thin films and subsequent annealing. We focus on the system Au-hematite because of the outstanding properties of each of the constituent elements. On the one hand, Au NPs exhibit intense optical activity associated to the surface plasmon resonance (SPR), chemical stability, high biocompatibility and easy functionalization^{1,16}. On the other hand, hematite presents low toxicity and intense photocatalytic activity¹⁷. Moreover, the combination of those components may exhibit additional features as enhanced photocatalytic activity for CO oxidation¹⁸ or coupling between magnetic and optical properties of the elements¹⁹ due to surface or proximity effects.

Au and Fe films were deposited onto silica substrates by thermal evaporation using a tungsten filament and Au and Fe wires as source in a home-made evaporation chamber. The vacuum in the chamber during the film deposition was 10^{-6} torr and the deposition rate was of 0.02 nm/s controlled with a Q-microbalance. The distance between the filament and the substrates was about 25 mm. The area of the substrate that can be coated with a metallic film is about 20x20 cm.

The temperature required for breaking the continuous thin films into nanostructures depends on the particular metal and substrates used¹². For Au films it is well reported in literature that NPs are formed upon annealing in the range 300°C-500°C. As the temperature increases, the NPs become larger, more separated and tend to acquire rounded shapes in order to reduce surface energy²⁰.

We initially studied the formation Fe oxide NPs from Fe films deposited onto silica substrates. We succeed on getting NPs upon annealing at 1100°C in air. Annealing at this temperature in air induces the total transformation of the Fe film into α -Fe₂O₃ hematite. As stated above, the formation of the nanoparticles from a continuous film is mechanically driven. The difference in thermal expansion coefficient between the film and the substrate induces stresses at the interface that are relieved breaking the film into NPs. The large difference between linear expansion coefficient of Au ($14 \cdot 10^{-6}$ °C⁻¹) and the silica ($0.6 \cdot 10^{-6}$ °C⁻¹) prompts the appearance of significant stresses and the formation of NPs at temperatures as low 300°C. While Fe has a thermal expansion coefficient similar to that of Au ($11.8 \cdot 10^{-6}$ °C⁻¹) it becomes oxidised in few minutes upon annealing above 150°C, a temperature too low to promote the formation of NPs. The thermal expansion coefficient of iron oxides is significantly smaller than that of the metals and consequently higher temperatures are required to achieve the strains needed for the formation of the NPs. Such stresses are only obtained above 900-1100°C for which iron has completely transformed into hematite.

Annealing in vacuum or reducing atmospheres in order to prevent iron oxidation is not a chance. The mass transport mechanism for the formation of NPs is mainly surface diffusion. The surface diffusion coefficient of metals is increased several orders of magnitude by the oxygen adsorbed on the metal surface. Actually annealing of Au films in vacuum induces the evaporation of the film prior to the formation of NPs. Therefore, we can not obtain the NPs following this method without oxidising the iron film.

The large difference in the temperatures required to obtain Au NPs (300°C-500°C) and α -Fe₂O₃ ones (900-1100°C) conditions the strategy to fabricate the hybrid nanostructures, since at 1000°C the Au film melts and evaporate. Thus, the first approach consisted on depositing a Fe film and anneals it to obtain the hematite NPs. Later, an Au film is deposited over the hematite NPs and a second annealing treatment is carried out. As the temperature of this second annealing is significantly smaller than the initial one, the hematite NPs does not suffer appreciable modifications during this process. In this way it is possible to control the morphology of both kinds of nanoparticles separately.

Figure 1 shows the characterization of a sample prepared following this approach, consisting on a 10 nm Fe thin film prepared by thermal evaporation annealed in air at 1050°C for 4 hours, plus a subsequent deposition of a 10 nm Au film and annealing in air for 3 hours at 500°C. The AFM image in figure 1a shows a bottom layer of NPs with average size in the range 50-200 nm and 20-70 nm height and a second type of NPs on top of the previous ones with average size about 500 nm and height of the order of 140-180 nm (see profile in figure 1b). Microraman analysis of the sample (figure 1c & 1d) confirmed the small NPs of the bottom layer to be hematite (α -Fe₂O₃)^{21,22}, and the large NPs on the top to be Au. Modifying the initial thickness of the films and the annealing conditions we are able to tune independently the morphology of the NPs and consequently their individual properties.

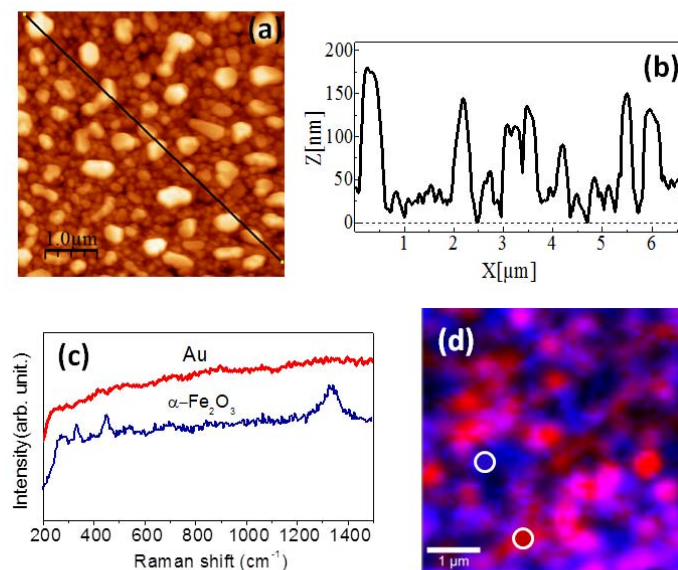


Figure1. Morphological and spectroscopy characterization for a sample prepared by a 10nm Fe film annealed in air at 1050°C 4h plus a 10 nm Au film annealed in air at 500°C for 3 hours. (a) AFM image, (b) height profile measured along the line indicated in the AFM image, (c) Raman spectra on the α -Fe₂O₃ and Au NPs, and (4) Raman image of a sample area, where blue and red points represent α -Fe₂O₃ and Au NPs respectively.

The Au NPs obtained over the hematite NPs layer results smaller than those obtained for an Au film with the same thickness deposited directly on the silica substrate. The discontinuous profile of the hematite film induces a more heterogeneous stress distribution than in a flat glass substrate, favouring the nucleation of holes, leading to smaller NPs.

Raman spectroscopy is a fast and non destructive tool to determine the quality of crystalline materials, including surface conditions and homogeneity. However, the samples oxidation can be modified depending on the laser power used. Due to this, XANES (X-ray Absorption Near Edge Structure) Fe K-edge measurements of the NPs were carried out. The figure 2 shows XANES spectra for the bulk references (Fe₃O₄, α -Fe₂O₃ and γ -Fe₂O₃) and for a sample prepared by a 10nm Fe film annealed in air at 1050°C 4h plus a 10 nm Au film annealed in air at 500°C for 3 hours. With the comparison of the XANES spectra we can confirm the oxidation state of NPs iron oxide as hematite.

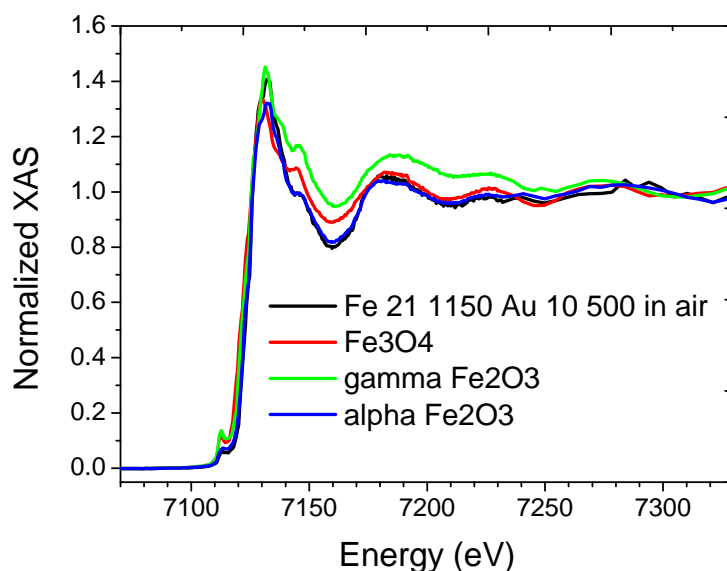


Figure2. XANES spectra for the bulk references (Fe₃O₄, α -Fe₂O₃ and γ -Fe₂O₃) and for a sample prepared by a 10nm Fe film annealed in air at 1050°C 4h plus a 10 nm Au film annealed in air at 500°C for 3 hours.

The coupling effects between the Au and hematite NPs can be enhanced upon the formation of dimmers with both components. The formation of these dimmers results quite difficult with the described approach in which each kind of NPs is processed in separated steps step and at fairly different temperatures. In order to promote the formation of these dimmers we used a second approach consisting on the deposition of Au/Fe bilayers and a subsequent annealing at high T. The covering Fe layer prevents the evaporation of the Au film and retards the formation of Au NPs by avoiding the absorption of oxygen on the Au surface. Then, it is possible to retain the Au on the substrate upon annealing at high temperatures in air.

Figure 3 shows two AFM samples fabricated with this approach varying the thickness of the Fe thin film and annealing time. The first sample was obtained growing an 10nm Au / 10 nm Fe bilayer plus a subsequent single annealing at 1200°C for 3 minutes. The AFM image (figure 3a) shows NPs with an average size in the range from 20 to 180 nm and a height between 100 and 500 nm (see roughness profile in figure 3c). A detailed analysis using phase contrast in AFM images (figure 3a inset), evidenced the formation of Au/hematite dimmers. A seconds sample was prepared from a 10nm Au / 20nm Fe bilayer and annealing at 1200°C for 30 minutes. In figure 3b, the corresponding AFM image shows NPs with an average size in the range from 200 to 500 nm and a height in the range of the 50-200 nm (see roughness profile in figure 3d). Inset in figure 3c present the AFM phase image where the formation of dimmers is evidenced although in this case both elements have a very similar size. Confocal Raman microscopy and XANES measurements (not shown) confirmed also the complex nature of the dimmers formed by Au and hematite NPs.

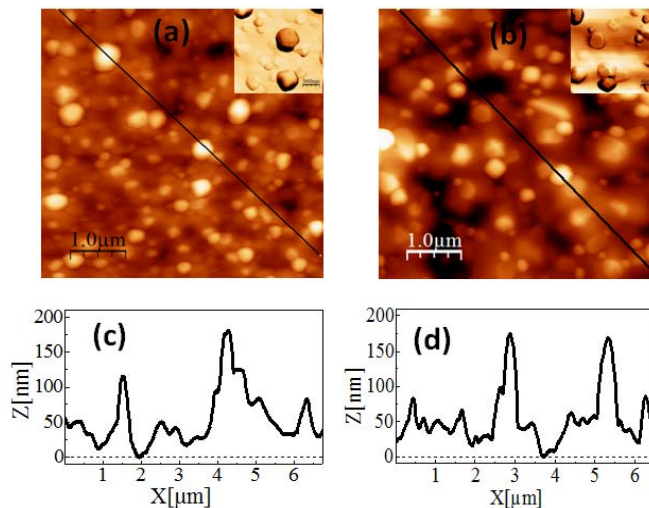


Figure 3. Morphological characterization for two sample obtained by Au/Fe bilayers annealed at 1200°C in air. Topography AFM images and insets that shows the phase images (a) of the Au/Fe bilayers of 10nm Au and 10nm Fe thickness annealed for 3 minutes, (b) of the Au/Fe bilayer of 10nm Au and 20nm Fe thickness annealed for 30 minutes and (c), (d) height profiles measured along the lines indicated in the AFM images.

As abovementioned, the only iron oxide phase we could obtain was hematite which exhibits an antiferromagnetic character, different to magnetite or maghemite that are ferromagnetic, showing consequently additional properties. It is well known that hematite can be reduced to magnetite by annealing and quenching²³. We tested this approach that allowed us to obtain Fe₃O₄, NPs, but they resulted detached from the substrate, so this approach neither results valid to obtain complex NPs.

Therefore, while this method does not allow a complete control of the morphology and structure of both species, it is possible to tune them at some extend. In contrast, the formation of dimmers enhances the coupling effects between both kinds of nanoparticles. Confirming this statement, figure 4 shows the optical absorption spectra of samples consisting on a 10 nm Au film and Fe layers with different thicknesses ranging from 2 to 10 nm. The absorption band associated to the surface plasmons resonance of Au NPs is clearly observed on the spectra. The width of this band is related to NP size but its position is determined by the surrounding medium. Hence, the shift observed as a function of the thickness of the initial Fe layer is a direct confirmation of the coupling of both kinds of NPs evidenced by the AFM images.

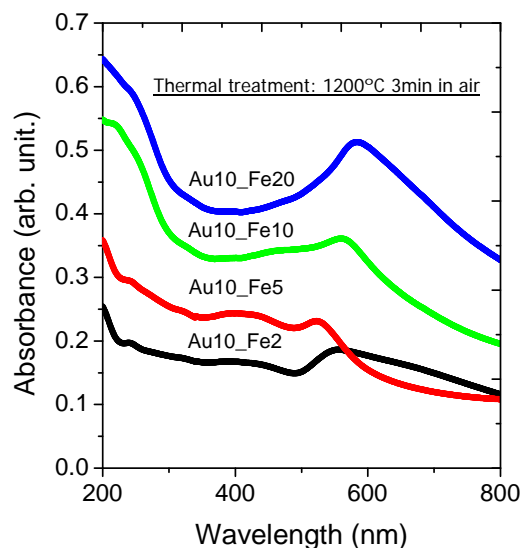


Figure 4. Optical absorption spectra for four sample obtained by Au/Fe bilayers annealed at 1200°C in air for 3min with different thickness of Fe thin films.

In summary, we have presented here a new method to fabricate large amounts of complex nanoparticles covering large (several centimetres) substrates by thin film deposition and annealing in air. Within this method there are different strategies that that allow tuning the morphology of the nanoparticles independently or promote the formation of complex dimmers to enhance the coupling effects. The method was successfully applied to the fabrication of Au-hematite NPs ensembles although it can be applied to a wide range of composed materials.

References

-
- ¹U. Kreibig and M. Vollmer, *Optical Properties of Metal Clusters*, Springer Series in Material Science Vol. 25 (Springer-Verlag, Berlin, 1995)
- ²A. P. Alivisatos, *Science*, **271**, 933 (1996)
- ³S. Chatterjee, A. Bandyopadhyay and K. Sarkar, *Journal of Nanobiotechnology*, 9:34 (2011)
- ⁴P. Tartaj, M. P. Morales, T. González-Carreño, S. Veintemillas-Verdaguer and C. J. Serna, *Adv. Mater.*, XX (2011)
- ⁵Y. Lee, M. A. Garcia, N. A. Frey Huls and S. Sun, *Angew. Chem. Int. Ed.*, **49**, 1271 (2010)
- ⁶M. Grzelczak, J. Pérez-Juste, P. Mulvaney and L. M. Liz-Marzán, *Chem. Soc. Rev.*, **37**, 1783 (2008)
- ⁷H. Ling Liu, J. Hua Wu, J. Hyun Min and Y. Keun Kim, *J. Appl. Phys.* **103**, 07D529 (2008)
- ⁸H.Y. Park, M. J. Schadt, L.Wang, I-lm S. Lim, P. N. Njoki, S. H. Kim, M.-Y. Jang, J. Luo, and C.J. Zhong, *Langmuir*, **23**, 9050 (2007)
- ⁹R. S. Kan, *Angew. Chem. Int. Ed.*, **47**, 1368 (2008)
- ¹⁰A. E. B. Presland, G. L. Price, and D. L. Trimm, *Surf. Sci.*, **29**, 424 (1972)
- ¹¹M. S. Rahman Khan, *Bull. Mater. Sci.*, **9**, 55 (1987)
- ¹²J. A. Thornton and D. W. Hoffman, *Thin Solid Films*, **171**, 5 (1989)
- ¹³I. Doron-Mor, Z. Barkay, N. Filip-Granit, A. Vaskevich, and I. Rubenstein, *Chem. Mater.*, **16**, 3476 (2004)
- ¹⁴S. Aggarwal, A. P. Monga, S. R. Perusse, R. Ramesh, V. Ballarotto, E. D. Williams, B. R. Chalamala, Y. Wei and R. H. Reuss, *Science*, **287**, 2235 (2000)
- ¹⁵S. R. Shinde, A. S. Ogale, S. B. Ogale, S. Aggarwal, V. Novikov, E. D. Williams and R. Ramesh, *Phys. Rev. B*, **64**, 035408 (2001)
- ¹⁶M A Garcia, *J. Phys. D: Appl. Phys.*, **44**, 283001 (2011)
- ¹⁷R. M. Conell and U. Schwertmann, *The iron oxides*, Wiley-VCH Verlag GmbH & Co. KGaA, Second Edition (Weinheim 2003)
- ¹⁸W. H. Hung, M. Ayko, D. Valley, W. Hou and S. B. Cronin, *Nano Lett.*, **10**, 1314 (2010)
- ¹⁹C. de Julián Fernández, G. Mattei, E. Paz, R. L. Novak, L. Cavigli, L. Bogani, F. J. Palomares, P. Mazzoldi and A. Caneschi, *Nanotechnology*, **21**, 165701 (2010)
- ²⁰A. Serrano. O. Rodriguez de la Fuente and M. A. Garcia, *J. Appl. Phys* **108**, 074303 (2010)
- ²¹H. Cao, G. Wang, L. Zhang, Y. Liang, S. Zhang and X. Zhang, *Chem. Phys. Chem*, **7**, 1897 (2006)
- ²²D. Bersani, P. P. Lottici and A. Montenero, *J. Raman Spectrosc.*, **30**, 355 (1999)
- ²³F. Kenfack and H. Langbein, *Cryst. Res. Technol.*, **39**, No. 12, 1070 (2004)